

The glucose-lowering effects of the PDE4 inhibitors roflumilast and roflumilast-*N*-oxide in *db/db* mice

S. Vollert · N. Kaessner · A. Heuser · G. Hanauer ·
A. Dieckmann · D. Knaack · H. P. Kley · R. Beume ·
C. Weiss-Haljiti

Received: 30 January 2012 / Accepted: 31 May 2012 / Published online: 13 July 2012
© Springer-Verlag 2012

Abstract

Aims/hypothesis The cAMP-degrading phosphodiesterase 4 (PDE4) enzyme has recently been implicated in the regulation of glucagon-like peptide-1 (GLP-1), an incretin hormone with glucose-lowering properties. We investigated whether the PDE4 inhibitor roflumilast elevates GLP-1 levels in diabetic *db/db* mice and whether this elevation is accompanied by glucose-lowering effects.

Methods Plasma GLP-1 was determined in *db/db* mice after single oral administration of roflumilast or its active metabolite roflumilast-*N*-oxide. Diabetes-relevant variables including HbA_{1c}, blood glucose, serum insulin, body weight, food and water intake, and pancreas morphology were determined in *db/db* mice treated daily for 28 days with roflumilast or roflumilast-*N*-oxide. Pharmacokinetic/pharmacodynamic analysis clarified the contribution of roflumilast vs its metabolite. In addition, the effect of roflumilast-*N*-oxide on insulin release was investigated in primary mouse islets.

Results Single treatment of *db/db* mice with 10 mg/kg roflumilast or roflumilast-*N*-oxide enhanced plasma GLP-1 2.5- and fourfold, respectively. Chronic treatment of *db/db* mice with roflumilast or roflumilast-*N*-oxide at 3 mg/kg showed prevention of disease progression. Roflumilast-*N*-oxide abolished the increase in blood glucose, reduced the increment in HbA_{1c} by 50% and doubled fasted serum insulin compared with vehicle, concomitant with preservation of pancreatic islet morphology. Furthermore, roflumilast-*N*-oxide amplified forskolin-induced insulin release in primary islets. Roflumilast-*N*-oxide showed stronger glucose-lowering effects than its parent compound, consistent with its greater effect on GLP-1 secretion and explainable by pharmacokinetic/pharmacodynamic modelling.

Conclusions/interpretation Our results suggest that roflumilast and roflumilast-*N*-oxide delay the progression of diabetes in *db/db* mice through protection of pancreatic islet physiology potentially involving GLP-1 and insulin activities.

Keywords Beta cells · GLP-1 · HbA_{1c} · Insulin · Intestine · Islets · Modelling · Obesity · Pharmacokinetic · PKPD

Abbreviations

COPD	Chronic obstructive pulmonary disease
EMAX	Maximum possible treatment effect on HbA _{1c}
GLP-1	Glucagon-like peptide-1
H&E	Haematoxylin and eosin
LLOQ	Lower limit of quantification
PD	Pharmacodynamic
PDE	Phosphodiesterase
PDE ₅₀	tPDE4i value leading to 50% of EMAX
PK	Pharmacokinetic
tPDE4i	Total PDE4 inhibition

S. Vollert (✉) · A. Heuser
Nycomed: a Takeda company, Nycomed GmbH,
Institute of Pharmacology and Preclinical Drug Safety,
Department RDP/LP,
Haidkrugsweg 1,
22885 Barsbüttel, Germany
e-mail: Stefanie.Vollert@takeda.com

N. Kaessner · G. Hanauer · A. Dieckmann · H. P. Kley ·
R. Beume · C. Weiss-Haljiti
Nycomed,
Konstanz, Germany

D. Knaack
Actelion Pharmaceuticals,
Allschwil, Switzerland

Introduction

Phosphodiesterases constitute a multigenic superfamily (PDE1–PDE11) that hydrolyse cAMP or cGMP and play a pivotal role in intracellular signalling pathways [1]. PDE4 selectively hydrolyses and inactivates cAMP. Its function in inflammatory cells was intensively studied [2] and research into PDE4 inhibitors has focused primarily on inflammatory disorders such as asthma and chronic obstructive pulmonary disease (COPD) [3]. Recent evidence suggests that PDE4 plays an essential role in glucose and fat metabolism [4–8]. PDE4B-deficient mice show reduced adiposity and decreased high-fat diet-induced adipose inflammation [4] and the PDE4 inhibitor rolipram protects mice on a high-fat diet against obesity and glucose intolerance [5]. A mild induction of glucose-dependent insulin release in response to roflumilast was presented *in vitro* [6], and enhanced glucagon-like peptide-1 (GLP-1) secretion in response to rolipram was recently shown in intestinal GLUTag cells and non-diabetic rats [7]. GLP-1 and insulin are central hormones in glucose metabolism and able to trigger glucose-lowering effects [9]. So far, PDE4 inhibitors have not been tested in animal models of type 2 diabetes and thus no information is available about their potential glucose-lowering properties. Hence we hypothesised that PDE4 inhibition might improve glucose homeostasis in a type 2 diabetes model including elevation of GLP-1 and insulin. In the present study we used *db/db* mice, a well-known model of type 2 diabetes [10], to evaluate the effect of the PDE4 inhibitor roflumilast on diabetes progression and potential changes in plasma GLP-1 and insulin. Roflumilast, a selective PDE4 inhibitor approved for treatment of COPD, is metabolised to the active metabolite roflumilast-*N*-oxide in humans. We included one treatment arm of roflumilast-*N*-oxide to assure efficacious plasma concentrations of the metabolite in the *db/db* mouse model.

Methods

Animals Female *db/db* mice (BKS.Cg-m^{+/+}Lepr^{db}/BomTac) were delivered by Taconic Europe (Lille Skensved, Denmark) at 5–6 weeks of age. The animals were housed in standard conditions (five animals/Makrolon cage type III, 12 h light–dark cycle) with free access to tap water and standard chow (no. 3433, Provimi Kliba, Kaiseraugst, Switzerland). Prior to inclusion in experiments, animals were randomised based on body weight and HbA_{1c}. All experiments were conducted according to the German Animal Protection Law and were approved by the local ethics committee.

Acute studies in *db/db* mice At 7 weeks of age, 16 h fasting mice received a single oral dose of vehicle (4% methocel) or

test compound (10 mg/kg roflumilast or roflumilast-*N*-oxide, maximal pharmacological effective dose without side effects following single administration), and a glucose bolus of 2 g/kg body weight was co-administered as a physiological initiator for GLP-1 secretion. The glucose concentration of 2 g/kg body weight was identified in pre-experiments as being optimal because it did not markedly induce GLP-1 levels on its own but potently triggered GLP-1 release in concert with our PDE4 inhibitors. Plasma GLP-1 was analysed 60 min before, and 10 and 60 min after administration of PDE4 inhibitor and glucose. The effect of roflumilast and roflumilast-*N*-oxide on plasma GLP-1 was also investigated in the absence of the glucose bolus.

Chronic study in *db/db* mice At 7 weeks of age, all animals were treated once daily by oral gavage with vehicle (4% methocel), roflumilast or roflumilast-*N*-oxide. Body weight and food and water intake were monitored daily. Animals destined for pharmacodynamic analysis (PD animals) were treated with roflumilast (0.3, 1 and 3 mg kg⁻¹ day⁻¹) or roflumilast-*N*-oxide (3 mg kg⁻¹ day⁻¹) for 28 days, with 3 mg/kg being the maximal pharmacological effective dose without side effects following chronic administration. HbA_{1c} was determined 6 days and 1 day before, and 14 and 28 days after treatment start. At days 1 and 28, an OGTT was performed for analysis of blood glucose and serum insulin. For OGTT, animals received a glucose bolus of 1 g/kg body weight after fasting for 4 h. In contrast to 16 h fasting in the acute study, the shorter 4 h fasting period results from method optimisation experiments we performed for ethical reasons and provides comparable results to those with 16 h fasting. Blood was collected 15 min before and 15 and 60 min after the glucose challenge. The glucose AUC was determined from time –15 to 60 min. Additional blood samples were taken at days 20 and 28 after treatment start for drug exposure analysis. Animals were killed by cervical dislocation on day 28 and the pancreas was removed for histopathological examination. For pharmacokinetic (PK) analysis, we included satellite animals (PK animals) which were treated with 3 mg kg⁻¹ day⁻¹ roflumilast or roflumilast-*N*-oxide for 34 days. At days 1, 14, 20, 34 and 35, blood samples were taken for drug exposure analysis.

Blood variables Blood samples were obtained from mouse tail vein or retro-orbital venous plexus during isoflurane anaesthesia. HbA_{1c} was determined by the latex agglutination inhibition method and plasma glucose by the glucose hexokinase method using an automated analyser ADVIA 1200 (Siemens Healthcare Diagnostics, Eschborn, Germany). Serum insulin was determined by ultrasensitive mouse insulin ELISA kit (Mercodia, Uppsala, Sweden). Plasma GLP-1 was determined by sandwich immunoassay with the Mouse/Rat GLP-1 (7-36)amide Assay Kit using the SECTOR 2400 Imager (Meso Scale Discovery, Gaithersburg, MD, USA). This kit detects amidated forms of GLP-1 including active and inactive GLP-1.

Histology and immunohistochemistry Pancreatic tissue was fixed in 4% neutral buffered formalin for 2 days and embedded in paraffin. Histological examination was standardised by selecting the main excretory exocrine ducts as anatomical landmarks. Accordingly, two longitudinal consecutive sections of 2 µm thickness including exocrine excretory ducts were processed from each animal and either stained with haematoxylin and eosin (H&E) or immunohistochemically for the insulin antigen to demonstrate the amount of beta cells. Immunohistochemical staining for insulin was performed on deparaffinised slides using the OptiMax Plus 2.0 autostainer system (BioGenex, San Ramon, CA, USA). Briefly, after antigen retrieval with enhancer solution (Histoprime, Linearis Biologische Produkte, Dossenheim, Germany, 15 min, 96°C) and blockage of endogenous peroxidase activity, guinea pig anti-insulin polyclonal antibody (Dakocytomation Hamburg, Germany, clone A564, diluted 1:3,000) was applied for 45 min followed by biotinylated anti-guinea pig antibody (Vector Laboratories, Burlingame, Canada, diluted 1:500) for 25 min and streptavidin horseradish peroxidase complex (DCS, BioGenex). Diaminobenzidine was used to visualise antibody binding, and haematoxylin for counterstaining.

Severity grading Islet atrophy degree was assessed by a certified pathologist on H&E slides blinded to treatment. Morphological features of pancreatic islets in *db/db* mice at different diabetic stages have been described [11]. Briefly, two types of islets were distinguished: enlarged well-demarcated round-shaped islets representing hypertrophic islets in the stage of increased insulin production by beta cells, and small irregular-shaped islets representing atrophic islets with decreased ability to secrete insulin. Based on these types, the degree of islet cell destruction was graded semi-quantitatively according to the percentage of atrophic islets in the section. Grading: minimal atrophy/grade 1 (less than 10% of islets affected), mild atrophy/grade 2 (≤25% of islets affected), moderate atrophy/grade 3 (≤50% of islets affected), marked atrophy/grade 4 (≤75% of islets affected) and severe/grade 5 (islets completely vanished).

PKPD analysis in chronic *db/db* mouse study Drug exposure was analysed in blood samples from PD and PK animals taken at different time points, with each animal providing two and eight samples, respectively (PD animals: −0.5/2 h, day 20; 30 h, day 28. PK animals: 0.5/1/2/4/8 h, day 1; 0.5/1/4 h, day 14; 0.5/2 h, day 20; −0.5/0.5/1/2/4/8 h, day 34; 30 h, day 35). Samples with values greater than the lower limit of quantification (LLOQ) were used for analysis (HPLC-MS/MS, LLOQ=0.5 µg/l) after roflumilast-*N*-oxide dosing, corresponding to 51 and 60 concentration values being available for parent and metabolite, respectively. After roflumilast dosing, 89 concentration values were available for both parent and metabolite, and values below LLOQ

were set to half LLOQ (0.25 µg/l) to reduce model bias. Four PK models were developed, that is for both roflumilast and its metabolite after both roflumilast and roflumilast-*N*-oxide dosing, respectively. All variables were estimated using the non-linear mixed-effects modelling (NONMEM) technique (version 7, ICON Development Solutions, Ellicott City, MD, USA) with first-order conditional estimation with interaction. From the obtained individual apparent clearance estimates, individual steady state AUC was calculated for each PD animal according to the following equation: $AUC (\mu\text{g h l}^{-1}) = \text{dose } (\mu\text{g/kg}) / \text{clearance } (\text{l h}^{-1} \text{ kg}^{-1})$. AUC estimates were used to determine total PDE4 inhibition (tPDE4i) of the respective compounds for all PD animals. The tPDE4i relates the average free concentration of a compound in plasma to its in vitro IC₅₀ of PDE4 inhibition, and is an exposure surrogate allowing for the consideration of parallel contribution of parent and metabolite to the overall effect. It is calculated as follows [12]:

$$tPDE4i = \frac{AUC_{rof} \cdot f_{u,rof}}{IC_{50,rof} \cdot \tau} + \frac{AUC_{rofNO} \cdot f_{u,rofNO}}{IC_{50,rofNO} \cdot \tau}$$

with *rof* and *rofNO* corresponding to roflumilast and roflumilast-*N*-oxide, f_u corresponding to the unbound fraction in mouse plasma in vitro, IC₅₀ corresponding to the compound concentration resulting in 50% PDE4 inhibition in vitro and τ corresponding to the dosing interval. To consider the presence of both roflumilast and roflumilast-*N*-oxide in the circulation, tPDE4i values calculated separately for each compound were added. The combined individual tPDE4i values were used as a measure of exposure in the subsequent PKPD model. HbA_{1c} levels on days −1, 14 and 28 from vehicle, roflumilast and roflumilast-*N*-oxide groups were used as PD readout, and were related to individual tPDE4i values using the following equation:

$$HbA_{1c} = H_0 + slope \cdot \left(1 - \frac{EMAX \cdot tPDE4i}{tPDE4i + PDE_{50}} \right) \cdot DAY$$

with H_0 corresponding to the estimated HbA_{1c} on day −1, slope corresponding to the steepness of HbA_{1c} increase over time, EMAX corresponding to the maximum possible treatment effect, DAY corresponding to the treatment day (day −1 defined as DAY=0) and PDE₅₀ being the tPDE4i leading to 50% of EMAX. The final PKPD model was evaluated by simulating new individual concentration–time profiles based on 200 simulations from the original dataset and the variable estimates from the final model. From all simulated observations, the median and the 5% and 95% quantiles were calculated for each time point and presented graphically together with all measured observations. All measured observations were compared with the corresponding 90% prediction interval.

Insulin secretion assay in isolated pancreatic islets For each experiment islets were isolated from four male c57BL/6

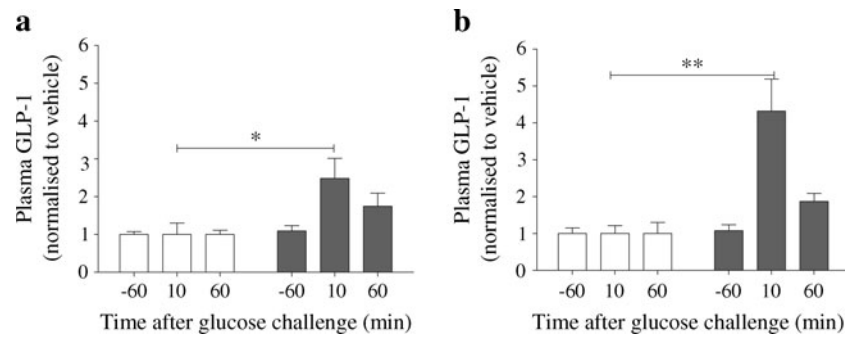


Fig. 1 Increase in plasma GLP-1 following acute administration of (a) roflumilast and (b) roflumilast-*N*-oxide in *db/db* mice. Seven-week-old fasting mice received a single administration of vehicle (white bars) or roflumilast and roflumilast-*N*-oxide (grey bars), respectively, at a dose of 10 mg/kg body weight together with a glucose bolus (2 g/kg body weight). Plasma GLP-1 levels were analysed 60 min before as well as

10 and 60 min after the glucose bolus. Plasma GLP-1 levels were normalised by dividing individual animal values through the corresponding mean value of vehicle-treated mice. Basal GLP levels of vehicle-treated animals were 11.8 and 9.7 pmol/l for (a) and (b), respectively. Data are presented as means \pm SEM ($n=10$ mice/group); * $p<0.05$, ** $p<0.01$ vs vehicle

mice, 6 weeks old, (Charles River Laboratories, Wilmington, MA, USA) using established methodology [13]. In summary, pancreases were removed by collagenase-supported surgery, further digested and a fat-free cell suspension mix containing intact islets was prepared by multiple centrifugation, filter steps and subsequent histopaque density centrifugation. For further purification, around 800 islets were picked with a 10 μ l pipette into culture medium and incubated overnight at 37°C and 5% CO₂ for recovery. The next day vital islets of defined size were selected using light microscopy and transferred into an ECM-coated 96-well plate resulting in five size-matched islets/well. Islets were incubated for two more days resulting in an adherent phenotype. For the glucose-stimulated insulin secretion assay islets were washed for 30 min and subsequently pre-incubated for another hour in KRH (1,150 mmol/l NaCl, 47.2 mmol/l KCl, 12 mmol/l MgSO₄ \times 7H₂O, 25.6 mmol/l CaCl₂ \times H₂O, 10 mmol/l HEPES, 0.5% BSA Fraction V) containing the basal glucose concentration of 2 mmol/l. Supernatants of each

individual well of the plate were preserved on ice for later determination of basal insulin secretion. Islets were stimulated with 10 mmol/l glucose either without or with the indicated compounds for 1 h in KRH. DMSO was equally 0.1% in all wells. After incubation, an aliquot of supernatant fraction ($n=4$ wells/stimulation condition) was taken for insulin quantification by ultrasensitive mouse insulin ELISA kit (Merckodia). Each sample was analysed in duplicate.

Statistical analysis Data are presented as mean \pm SEM or \pm SD. Multiple comparisons between groups were conducted by one-way ANOVA. A p value of <0.05 was considered significant.

Materials Roflumilast and roflumilast-*N*-oxide were synthesised by Nycomed medicinal chemistry (Nycomed, Konstanz, Germany). Methocel (methylcellulose, E15) was purchased from Dow Chemical (Dow Chemical, Midland, MI, USA) and glucose solutions from Serag Wiessner (Naila, Germany).

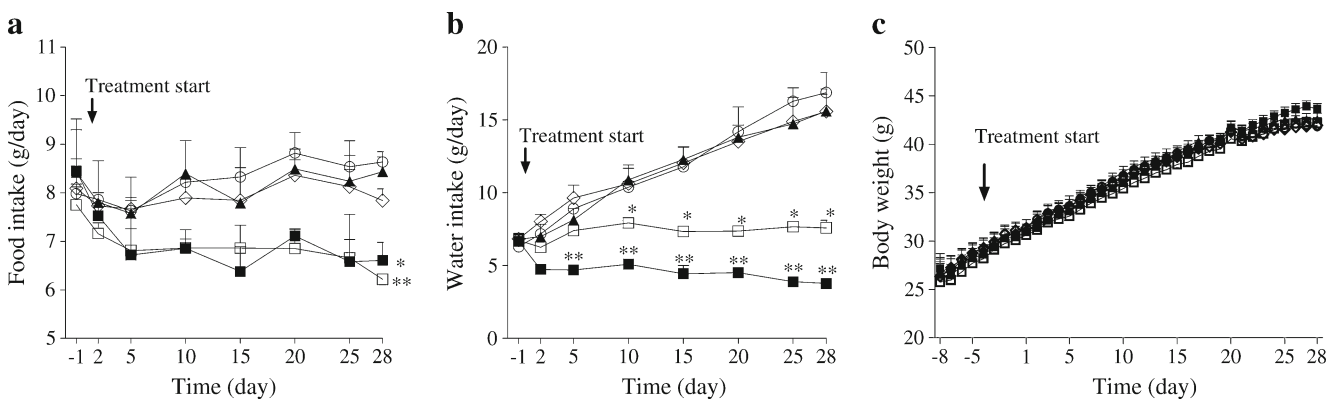


Fig. 2 Chronic effect of roflumilast and roflumilast-*N*-oxide on (a) food and (b) water consumption and on (c) body weight in *db/db* mice. Animals received an oral dose of vehicle (black triangles), roflumilast at a dose of 0.3 mg kg⁻¹ day⁻¹ (white circles), 1 mg kg⁻¹ day⁻¹ (white diamonds) and 3 mg kg⁻¹ day⁻¹ (white squares), or roflumilast-*N*-oxide

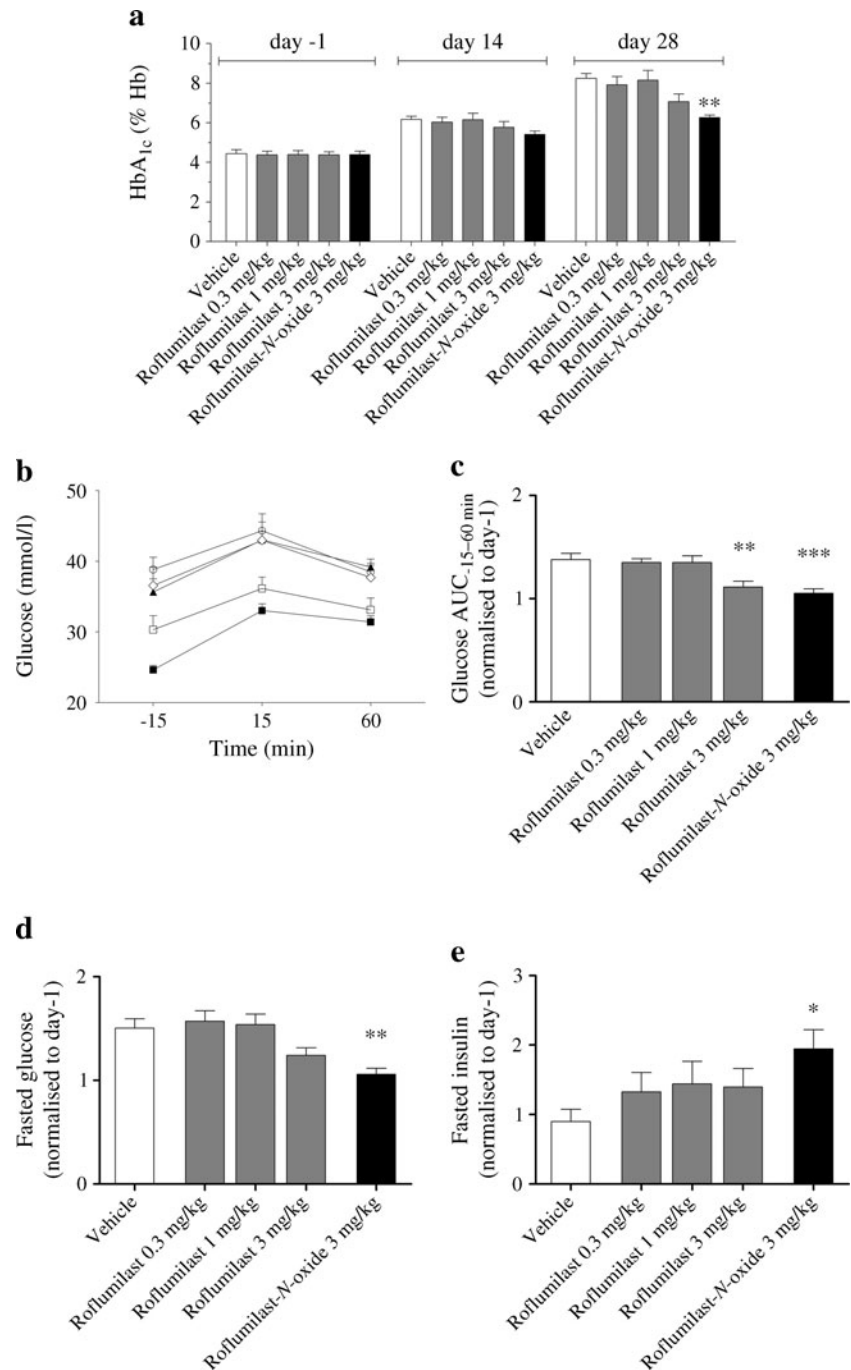
at a dose of 3 mg kg⁻¹ day⁻¹ (black squares) once daily for 28 days. Body weight and food and water consumption were measured daily during the treatment period. Data are presented as means \pm SEM ($n=10$ mice/group); * $p<0.05$ and ** $p<0.01$ vs vehicle

Results

Effect of single administration of roflumilast and roflumilast-*N*-oxide on plasma GLP-1 We investigated the effect of a single dose of 10 mg/kg roflumilast or roflumilast-*N*-oxide on plasma GLP-1 in fasted *db/db* mice. The PDE4 inhibitor's effect on plasma GLP-1 was investigated in the presence and absence of a glucose bolus as a physiological initiator of GLP-1 secretion. In the

presence of glucose, roflumilast and roflumilast-*N*-oxide significantly increased plasma GLP-1 by a factor of 2.5 and 4.3 vs vehicle, respectively (Fig. 1). The increase in plasma GLP-1 was observed 10 min after administration of PDE4 inhibitor and glucose, and was reversed 60 min after administration. In the absence of glucose, treatment with roflumilast or roflumilast-*N*-oxide resulted in minor insignificant increases of plasma GLP-1 (data not shown).

Fig. 3 Improvement of HbA_{1c}, blood glucose and serum insulin following chronic treatment with roflumilast and roflumilast-*N*-oxide in *db/db* mice. Animals received an oral dose of vehicle, roflumilast (0.3, 1 or 3 mg/kg) or roflumilast-*N*-oxide (3 mg/kg) once daily for 28 days. HbA_{1c}, blood glucose and serum insulin levels were measured at day -1 and day 28 in 4 h fasting *db/db* mice during an OGTT. HbA_{1c} was also measured in non-fasting animals at day 14. **(a)** HbA_{1c} development from day -1 to day 28. **(b)** Blood glucose at day 28 before and after glucose stimulation following treatment with vehicle (black triangles), roflumilast at 0.3 mg kg⁻¹ day⁻¹ (white circles), 1 mg kg⁻¹ day⁻¹ (white diamonds) or 3 mg kg⁻¹ day⁻¹ (white squares) or roflumilast-*N*-oxide at 3 mg kg⁻¹ day⁻¹ (black squares) and corresponding **(c)** glucose AUC₋₁₅₋₆₀, **(d)** fasting glucose and **(e)** fasting insulin, normalised to day -1. For normalisation, individual animal data at day 28 were divided through their corresponding values at day -1. Data are presented as means±SEM (*n*=10 mice/group); **p*<0.05, ***p*<0.01 and ****p*<0.001 vs vehicle. To convert values for HbA_{1c} in % into mmol/mol, subtract 2.15 and multiply by 10.929



Effect of chronic administration of roflumilast and roflumilast-*N*-oxide on body weight and food and water intake In *db/db* mice, roflumilast and roflumilast-*N*-oxide at 3 mg kg⁻¹ day⁻¹ reduced food and water consumption compared with vehicle (Fig. 2a, b). Average food consumption over 4 weeks was reduced by about 17% compared with vehicle after treatment with roflumilast or roflumilast-*N*-oxide. Water consumption increased during the study period from 6.7 g/day to 15.6 g/day in vehicle-treated animals and declined to 7.6 g/day and 3.8 g/day after 4 weeks of treatment with roflumilast and roflumilast-*N*-oxide, respectively. The effect on food and water consumption occurred right after the first administration and persisted for the whole study period. Roflumilast and roflumilast-*N*-oxide showed no effect on body weight (Fig. 2c).

Effect of chronic administration of roflumilast and roflumilast-*N*-oxide on blood variables In vehicle-treated animals, HbA_{1c} almost doubled from 4.4% (24.6 mmol/mol) to 8.2% (66.1 mmol/mol) within 4 weeks. Treatment with 3 mg kg⁻¹ day⁻¹ roflumilast and roflumilast-*N*-oxide reduced the increase in HbA_{1c}. The effect was visible after 2 weeks of treatment and resulted in a 50% reduction compared with vehicle after 4 weeks of treatment with roflumilast-*N*-oxide ($p < 0.01$) (Fig. 3a). Concomitant with HbA_{1c} development, blood glucose increased in vehicle-treated animals (Fig. 3b) by 38% and 51% with respect to glucose AUC₋₁₅₋₆₀ (Fig. 3c) and fasted glucose (Fig. 3d) at day 28. Roflumilast-*N*-oxide lowered glucose AUC₋₁₅₋₆₀ ($p < 0.001$ vs vehicle) and fasting blood glucose ($p < 0.01$ vs vehicle) to levels as low as at study start, whereas the effect with roflumilast was only significant for glucose AUC₋₁₅₋₆₀ ($p < 0.01$ vs vehicle) (Fig. 3b–d). Fasted serum insulin slightly decreased in vehicle-treated animals from 602 pmol/l at day -1 to 551 pmol/l at day 28. Roflumilast-*N*-oxide at 3 mg kg⁻¹ day⁻¹ almost doubled fasted serum insulin following 4 weeks of treatment ($p < 0.05$ vs vehicle). The effect of roflumilast on fasted serum insulin was less pronounced and not significant (Fig. 3e). Glucose-stimulated serum insulin levels did not increase but rather declined 15 min after glucose stimulation in vehicle- and PDE4i-treated animals (data not shown).

Effect of chronic administration of roflumilast and roflumilast-*N*-oxide on pancreatic morphology Histopathological examination of H&E stained slides showed mild to moderate islet atrophy in 11-week-old vehicle-treated *db/db* mice. The percentage of atrophic islets ranged between 25% and 50%, resulting in an islet atrophy severity grade of 2.6 (Fig. 4). Insulin staining on serial sections demonstrated that islet atrophy was associated with a loss of insulin-producing beta cells (Fig. 5a, b). Treatment with 3 mg/kg roflumilast or roflumilast-*N*-oxide once daily for 4 weeks preserved pancreatic islet morphology and insulin production in beta cells (Fig. 5c, d), resulting in mild (severity grade 2.0, $p > 0.05$ vs vehicle) and minimal (severity grade 1.3,

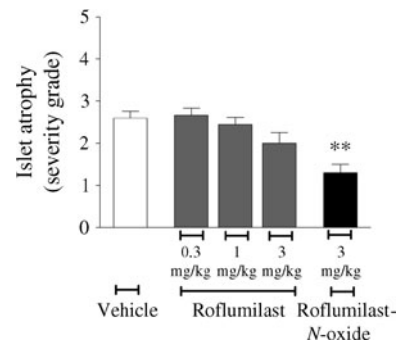


Fig. 4 Atrophy of pancreatic islets in *db/db* mice subsequent to oral treatment with vehicle, roflumilast (0.3, 1 or 3 mg/kg) or roflumilast-*N*-oxide (3 mg/kg) once daily for 28 days. Islet atrophy was assessed histopathologically on H&E slides. Semiquantitative analysis of morphological changes showed mild to moderate islet atrophy in vehicle-treated animals, which was ameliorated to mild and minimal atrophy following treatment with 3 mg/kg roflumilast and roflumilast-*N*-oxide, respectively. Data are shown as mean \pm SEM ($n = 10$ mice/group), ** $p < 0.01$ vs vehicle

$p < 0.01$ vs vehicle) islet atrophy for roflumilast and roflumilast-*N*-oxide, respectively (Fig. 4).

PKPD analysis of chronic *db/db* mouse study The PK of both roflumilast and roflumilast-*N*-oxide after roflumilast and roflumilast-*N*-oxide dosing, respectively, are best described by two-compartmental model structures with first-order absorption and elimination. The final AUC values for roflumilast and roflumilast-*N*-oxide were derived from the final respective PK model (Table 1). After roflumilast administration, AUC levels of the metabolite reached 67% of those of the

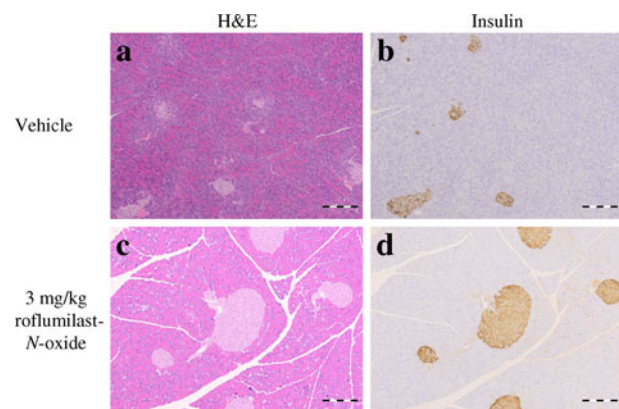


Fig. 5 Histopathological evaluation of pancreatic sections from *db/db* mice treated with vehicle or 3 mg/kg roflumilast-*N*-oxide once daily for 4 weeks. A whole pancreas was fixed, and consecutive sections were stained with H&E or anti-insulin antibody. Immunoreactive cells are labelled brown, counterstain with haematoxylin. Representative islets from each group are shown at magnification $\times 10$. Vehicle-treated animals showed (a) atrophy of pancreatic islets associated with (b) loss of insulin-producing beta cells. (c) Islet atrophy was prevented following treatment with roflumilast-*N*-oxide concomitant with (d) maintenance of insulin-producing beta cells. Scale bars = 200 μ m

Table 1 AUC and corresponding tPDE4i values for PD animals in chronic *db/db* mouse study

Administered compound and dose per day	Roflumilast		Roflumilast- <i>N</i> -oxide		Combined
	AUC (μg h/l)	tPDE4i _{rof}	AUC (μg h/l)	tPDE4i _{rofNO}	tPDE4i
Roflumilast, 0.3 mg/kg	136 (104–178)	0.744 (0.568–0.974)	86.9 (83.7–90.2)	0.731 (0.704–0.759)	1.49 (1.27–1.74)
Roflumilast, 1 mg/kg	408 (363–459)	2.23 (1.98–2.51)	275 (268–282)	2.31 (2.25–2.37)	4.55 (4.25–4.86)
Roflumilast, 3 mg/kg	1,201 (1,170–1,233)	6.56 (6.39–6.73)	853 (844–863)	7.18 (7.10–7.26)	13.8 (13.5–14.0)
Roflumilast- <i>N</i> -oxide, 3 mg/kg	68.6 (57.5–81.8)	0.375 (0.314–0.447)	2,633 (2,500–2,772)	22.1 (21.0–23.3)	22.5 (21.4–23.7)

Data are presented as geometric means (68% range)

tPDE4i values were calculated using f_u and IC_{50} values of 3.7% and 0.282 μg/l for roflumilast and 12.7% and 0.629 μg/l for roflumilast-*N*-oxide, respectively (N. Kaessner, unpublished data)

tPDE4i_{rof} and tPDE4i_{rofNO} correspond to the separate tPDE4 inhibition of roflumilast and roflumilast-*N*-oxide in the circulation, whereas the combined value considers the contribution of both compounds and was calculated from the individual combinations of tPDE4i_{rof} and tPDE4i_{rofNO}

Animals received roflumilast (0.3, 1 or 3 mg kg⁻¹ day⁻¹) or roflumilast-*N*-oxide (3 mg kg⁻¹ day⁻¹) once daily for 28 days

parent compound, and the extent of metabolite formation was the same for all doses. After administration of roflumilast-*N*-oxide, 2.6% was metabolised back into roflumilast. When transforming the AUC values into tPDE4i values, values for parent and metabolite were almost equal after roflumilast dosing. In contrast, the contribution of roflumilast to the overall effect after roflumilast-*N*-oxide dosing can be considered as marginal, as tPDE4i for roflumilast reached only 1.7% of tPDE4i for roflumilast-*N*-oxide. The combined tPDE4i for roflumilast and roflumilast-*N*-oxide was 1.6-fold higher following roflumilast-*N*-oxide dosing compared with roflumilast dosing (Table 1).

The final PKPD model variables are shown in Table 2. Interindividual variability was identified for H_0 , slope and PDE_{50} . All variables were estimated with good precision with relative standard errors <50%. H_0 started at 4.35% and was estimated to increase by 0.138% per day. The model

Table 2 Variable estimates of the final PKPD model

Model variable	Unit	Estimate	Relative standard error, %
H_0	%	4.35	1.25
Slope	%/day	0.138	4.80
EMAX	–	1.00	6.27
PDE_{50}	–	27.1	25.2
Interindividual variability			
ω_{H_0}	CV%	12.7	11.8
ω_{slope}	CV%	21.4	30.2
$\omega_{PDE_{50}}$	CV%	79.8	44.5
Residual variability			
Proportional	CV%	3.87	29.3

ω corresponds to interindividual variability, obtained using an exponential error model

Relative standard errors of variability variables are given on the variance scale. (–) in the unit column indicates that there are no units for this value

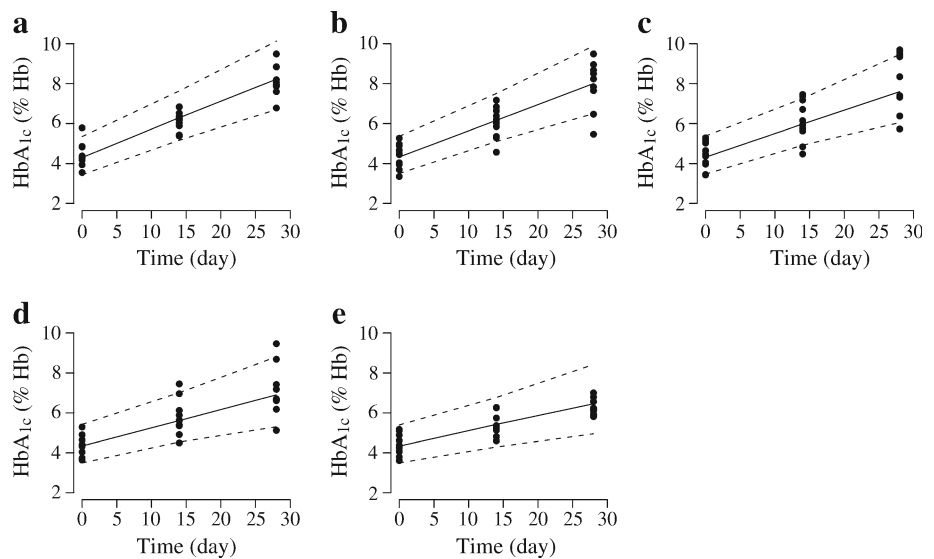
estimated that the maximum expected treatment effect would keep HbA_{1c} at its starting value. The PDE_{50} was estimated to be 27.1. A tPDE4i value of 27.1 would be reached with a roflumilast dose of 5.9 mg/kg. The graphical model evaluation is presented in Fig. 6. The estimated variables were well suited to describe the HbA_{1c} time course of all dose groups.

*Roflumilast-*N*-oxide amplifies insulin secretion in mouse islets* We examined elevated insulin secretion in response to roflumilast-*N*-oxide in primary mouse islets (Fig. 7). Forskolin, a broad activator of adenylyl cyclases thereby increasing intracellular cAMP, induced insulin secretion fourfold in mouse islets. The response to 1 μmol/l forskolin was synergistically enhanced with either 10 or 100 nmol/l roflumilast-*N*-oxide at 10 nmol/l glucose leading to a 5.5- or 7-fold increase in insulin release, respectively. Roflumilast (data not shown) and roflumilast-*N*-oxide without a co-stimulus were unable to induce insulin secretion in primary mouse islets at various tested glucose conditions (data shown for 100 nmol/l roflumilast-*N*-oxide at 10 mmol/l glucose).

Discussion

To our knowledge, we have shown for the first time the effect of PDE4 inhibition in an animal model of type 2 diabetes evaluating disease progression in detail and analysing the effects on GLP-1 and insulin being central hormones in glucose metabolism. Roflumilast was used as a selective PDE4 inhibitor, previously approved as a drug for the treatment of COPD. A recent human study with roflumilast addressed the question of efficacy in type 2 diabetes (E.F.M. Wouters, Maastricht University Medical Center, Maastricht, the Netherlands, unpublished results). In humans, roflumilast is metabolised to the active metabolite roflumilast-*N*-oxide, which exhibits a nearly 10-fold higher exposure compared

Fig. 6 Graphical evaluation of the final PKPD model, considering doses of (a) vehicle, (b) 0.3 mg/kg roflumilast, (c) 1 mg/kg roflumilast, (d) 3 mg/kg roflumilast or (e) 3 mg/kg roflumilast-*N*-oxide once daily for 28 days and HbA_{1c} as pharmacodynamic readout. Filled circles correspond to measured values of HbA_{1c}. The solid and dashed lines represent the median model prediction and the 90% prediction interval, respectively. The PKPD model captured the HbA_{1c} time course well over all dose groups. A reduction in HbA_{1c} can be observed for roflumilast (3 mg/kg) and roflumilast-*N*-oxide (3 mg/kg)



with its parent compound and acts as the principal contributor to the roflumilast drug effect [14]. As roflumilast metabolism in *db/db* mice was unknown, we included one treatment arm with roflumilast-*N*-oxide to assure efficacious plasma concentrations.

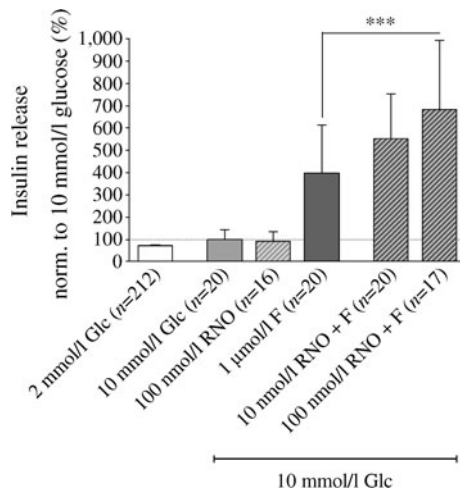


Fig. 7 Insulin secretion in primary mouse pancreatic islets is amplified by roflumilast-*N*-oxide (RNO). Islets were isolated from pancreases and five size-matched islets per well ($n=1$) were grown confluent for 2 days in a 96-well plate (48 central wells were used per plate). For the glucose-stimulated insulin secretion assay, islets of the entire plate were initially washed and pre-incubated in 2 mmol/l glucose (Glc) to determine the basal insulin secretion under basal glucose conditions, the mean is shown as a white bar on the left side. Islets were stimulated with 10 mmol/l Glc alone or in combination with the indicated amounts of compounds; 100 nmol/l RNO, 1 μ mol/l of the broad adenylyl cyclase activator forskolin (F) or combinations of both. Data were generated in four to five independent experiments, n corresponds to the number of individual wells, typically four wells were used per tested condition. Data are presented as means \pm SD; *** $p < 0.001$. Norm., normalized

In accordance with the previously reported GLP-1 elevating effect of rolipram in non-diabetic rats [7], we now confirm the result in a type 2 diabetes model. In diabetic *db/db* mice, single oral administration of 10 mg/kg roflumilast or its metabolite increased plasma GLP-1 vs vehicle in the presence of glucose by a factor of 2.5 and 4.3, respectively. As this report showed in addition that rolipram is able to directly stimulate the cAMP-mediated GLP-1 release in GLUTag cells, we concluded that the observed increase of GLP-1 in response to roflumilast results from cAMP-mediated GLP-1 release in intestinal L-cells of the *db/db* mice. In the absence of glucose, roflumilast and roflumilast-*N*-oxide had no significant effect on plasma GLP-1 suggesting that PDE4 inhibition amplifies GLP-1 release only following food intake, which is the physiological initiator of GLP-1 secretion [15]. In contrast, therapeutic GLP-1 mimetics elevate GLP-1 levels independent of food intake [16].

Chronic treatment of *db/db* mice with roflumilast or roflumilast-*N*-oxide clearly ameliorated the diabetic status of the animals. Roflumilast-*N*-oxide at 3 mg kg⁻¹ day⁻¹ almost abolished the increase in glucose AUC and fasting glucose over the study time and reduced the increment in HbA_{1c} by about 50% vs vehicle. In addition, fasted serum insulin levels almost doubled following 4 weeks of treatment concomitant with amelioration of pancreatic islet morphology and preservation of insulin production in beta cells. The improved diabetic status was also reflected by a reduction in water and, although less pronounced, food consumption relative to control. Water consumption decreased to 3.8 g/day, a level we observed in healthy mice (data not shown), suggesting that the renal glucose reabsorption capacity was no longer overloaded in contrast to vehicle-treated mice showing a high water intake of 15.6 g/day at the end of the study. Despite its food-reducing effect, roflumilast-*N*-oxide had no effect on body weight development. However, this discrepancy might be a *db/db*

mouse-specific effect as PDE4 inhibitors have been shown to reduce body weight in diet-induced obesity mice [5] and diabetic COPD patients [17]. This indicates that PDE4 inhibitors might be advantageous over current glucose-lowering drugs such as insulin, sulfonylureas or thiazolidinones, for which body weight gain is often an adverse event [18–20].

Compared with its parent roflumilast, chronic roflumilast-*N*-oxide treatment resulted in stronger glucose-lowering effects as demonstrated by a greater reduction of blood glucose and HbA_{1c} and superior islet preservation. The effect on food intake was similar for both compounds; however, this may be attributed to the limited sensitivity of the method. The stronger glucose-lowering effect of roflumilast-*N*-oxide following chronic treatment is consistent with its greater GLP-1-increasing effect following acute treatment. This observation and extensive published literature regarding the glucose-lowering role of GLP-1 [9, 21–27] support the view that roflumilast-mediated GLP-1 elevation and the prevention of diabetes progression in our *db/db* mice are linked. In particular, treatment of *db/db* mice with GLP-1 mimetics shows parallels to our study results with respect to reduced food and water consumption and preservation of pancreatic islets [28]. Another observation was striking to us, supporting our interpretation that PDE4 inhibitors ameliorate diabetes likely via enhancement of physiological intestinal GLP-1 release. Comparing drug reaction profiles of GLP-1 mimetics and PDE4 inhibitors in humans shows that both treatments can reduce body weight and cause gastrointestinal side effects such as delayed gastric emptying, transient nausea and diarrhoea [17, 29].

A reason for the stronger glucose-lowering effect of roflumilast-*N*-oxide compared with roflumilast is given by PK modelling as shown by a 1.6-fold higher value of the combined exposure surrogate tPDE4i after roflumilast-*N*-oxide treatment compared with treatment with the parent roflumilast. Furthermore, the modelling results suggest that PDE4 inhibitors carry the potential to keep HbA_{1c} at starting levels in *db/db* mice based on the estimated EMAX of 1. As the estimated PDE₅₀ of 27.1 in *db/db* mice is approximately 27-fold higher than the tPDE4i of 1.03 in humans at the effective dose of 500 µg [30], *db/db* mice seem to require higher exposures for efficacy than humans. This should be considered in the translation of results from mice to humans.

In addition to their intestinal action, PDE4 inhibitors probably act systemically, which is supported by PKPD modelling showing correlation of the systemic exposure surrogate tPDE4i and HbA_{1c} improvement. It is likely that the most important systemic area of action is the pancreas where PDE4 inhibitors might act in synergy with GLP-1 leading to enhanced insulin secretion. As vehicle-treated *db/db* mice did not show glucose-stimulated insulin secretion during OGTT explainable by the stage of hyperinsulinaemia

and beta cell condition, both depending on various factors such as breeder, age and sex, we addressed this question *ex vivo* in primary mouse islets. Our results indicate that roflumilast-*N*-oxide is able to synergise with adenylyl cyclase activation in the induction of insulin release, which was achieved in our hands by forskolin but can also occur in response to GPCR agonists such as GLP-1 (C. Weiss-Haljtiti, unpublished observations). Hence the PDE4 inhibitor may boost insulin secretion, acting directly on pancreatic islets and amplifying an insulin-secretory response to GLP-1, inhibitors of dipeptidyl peptidase IV or other triggers. These and other still less understood mechanisms are likely to play an important role in the preservation of beta cell mass supported by our islet morphology results. However, further studies are needed to investigate the mechanisms by which PDE4 inhibitors might prevent diabetes progression, in particular regarding cytokines, adipokines, insulin signalling components and insulin sensitivity of peripheral tissue.

In conclusion, our results suggest that chronic treatment with PDE4 inhibitors delays the progression of diabetes in *db/db* mice by improvement of glycaemic variables and protection of pancreatic islets. The occurring mechanisms such as enhanced intestinal GLP-1 secretion and amplification of the insulin-secretory response in the pancreas are leading to novel and promising combination concepts for treating type 2 diabetes.

Acknowledgements Expert technical assistance of B Friggemann, K Lagerpusch, N Schwagarus (Nycomed, a Takeda company, Nycomed, Barsbüttel, Germany) and M Ohme (Nycomed, a Takeda company, Nycomed, Konstanz, Germany) is gratefully acknowledged.

Duality of interest The authors are employees of Nycomed, a Takeda company, or Actelion Pharmaceuticals.

Contribution statement SV, NK and AH contributed to conception and design, data acquisition, analysis and interpretation, and drafting and revision of the article. GH and AD contributed to conception and design, data interpretation and revision of the article. DK contributed to conception and design, data acquisition, analysis and interpretation, and revision of the article. HPK and RB contributed to conception, data interpretation and revision of the article. CW-H contributed to conception and design, data acquisition, analysis and interpretation, and drafting and revision of the article. All co-authors approved the final version of the manuscript.

References

1. Lugnier C (2006) Cyclic nucleotide phosphodiesterase (PDE) superfamily: a new target for the development of specific therapeutic agents. *Pharmacol Ther* 109:366–398
2. Hatzelmann A, Morcillo EJ (2010) The preclinical pharmacology of roflumilast – a selective, oral phosphodiesterase 4 inhibitor in development of chronic obstructive pulmonary disease. *Pulm Pharmacol Ther* 23:235–256

3. Souness JE, Aldous D, Sargent C (2000) Immunosuppressive and anti-inflammatory effects of cyclic AMP phosphodiesterase (PDE) type 4 inhibitors. *Immunopharmacology* 47:127–162
4. Zhang R, Maratos-Flier E, Flier JS (2009) Reduced adiposity and high-fat diet-induced adipose inflammation in mice deficient for phosphodiesterase 4B. *Endocrinology* 150:3076–3082
5. Park SJ, Ahmad F, Philp A et al (2012) Resveratrol ameliorates aging-related metabolic phenotypes by inhibiting cAMP phosphodiesterases. *Cell* 148:421–433
6. Waddleton D, Wu W, Feng Y et al (2008) Phosphodiesterase 3 and 4 comprise the major cAMP metabolizing enzymes responsible for insulin secretion in INS-1 (832/13) cells and rat islets. *Biochem Pharmacol* 76:884–893
7. Ong WK, Gribble FM, Reimann F et al (2009) The role of the PDE4D cAMP phosphodiesterase in the regulation of glucagon-like peptide-1 release. *Br J Pharmacol* 157:633–644
8. Omar B, Zmuda-Trzebiatowska E, Manganiello V, Göransson O, Degerman E (2009) Regulation of AMP-activated protein kinase by cAMP in adipocytes: roles for phosphodiesterases, protein kinase B, protein kinase A, Epac and lipolysis. *Cell Signal* 21:760–766
9. Drucker DJ (2006) The biology of incretin hormones. *Cell Metab* 3:153–165
10. Hummel KP, Dickie MM, Coleman DL (1966) Diabetes, a new mutation in the mouse. *Science* 153:1127–1128
11. Yamazaki M, Kato A, Kato C et al (2009) Segmentation of the pathophysiological stages of diabetic changes in the db/db mouse. *J Toxicol Pathol* 22:133–137
12. Lahu G, Hünemeyer A, Herzog R et al (2009) Effect of repeated dose of erythromycin on the pharmacokinetics of roflumilast and roflumilast N-oxide. *Int J Clin Pharmacol Ther* 47:236–245
13. Rützi S, Ehses JA, Sibler RA et al (2009) Low- and high-density lipoproteins modulate function, apoptosis, and proliferation of primary human and murine pancreatic beta-cells. *Endocrinology* 150:4521–4530
14. Bethke TD, Böhmer GM, Hermann R et al (2007) Dose-proportional intraindividual single- and repeated-dose pharmacokinetics of roflumilast, an oral, once-daily phosphodiesterase 4 inhibitor. *J Clin Pharmacol* 47:26–36
15. Gribble FM (2008) RD Lawrence Lecture 2008: targeting GLP-1 release as a potential strategy for the therapy of type 2 diabetes. *Diabet Med* 25:889–894
16. Lund A, Knop FK, Vilsbøll T (2011) Emerging GLP-1 receptor agonists. *Expert Opin Emerg Drugs* 16:607–618
17. Rabe K (2011) Update on roflumilast, a phosphodiesterase 4 inhibitor for the treatment of chronic obstructive pulmonary disease. *Br J Pharmacol* 163(1):53–67
18. Dailey GE, Noor MA, Park JS, Bruce S, Fiedorek FT (2004) Glycemic control with glyburide/metformin tablets in combination with rosiglitazone in patients with type 2 diabetes: a randomized double-blind trial. *Am J Med* 116:223–229
19. Inzuchi SE (2002) Oral antihyperglycemic therapy for type 2 diabetes. *JAMA* 287:360–372
20. UK Prospective Diabetes Study Group (1998) UKPDS 24: a 6-year, randomized, controlled trial comparing sulfonylurea, insulin, and metformin therapy in patients with newly diagnosed type 2 diabetes that could not be controlled with diet therapy. *Ann Intern Med* 128:165–175
21. Fehmman HC, Habener JF (1992) Insulinotropic hormone glucagon-like peptide-I(7-37) stimulation of proinsulin gene expression and proinsulin biosynthesis in insulinoma beta TC-1 cells. *Endocrinology* 130:159–166
22. D'Alessio DA, Kahn SE, Leusner CR, Ensinnck JW (1994) Glucagon-like peptide-1 enhances glucose tolerance both by stimulation of insulin release and by increasing insulin-independent glucose disposal. *J Clin Invest* 93:2263–2266
23. Buteau J, El-Assaad W, Rhodes CJ, Rosenberg CJ, Joly E, Prentki M (2004) Glucagon-like peptide-1 prevents beta cell glucolipototoxicity. *Diabetologia* 47:806–815
24. Tourrel C, Bailbe D, Lacombe M, Meile MJ, Kergoat M, Portha B (2002) Persistent improvement of type 2 diabetes in the Goto-Kakizaki rat model by expansion of the β -cell mass during the prediabetic period with glucagon-like peptide-1 or exendin-4. *Diabetes* 51:1443–1452
25. Stoffers DA, Kieffer TJ, Hussain MA et al (2000) Insulinotropic glucagon-like peptide 1 agonists stimulate expression of homeodomain protein IDX-1 and increase islet size in mouse pancreas. *Diabetes* 49:741–748
26. Xu G, Stoffers DA, Habener JF, Bonner-Weir S (1999) Exendin-4 stimulates both β -cell replication and neogenesis, resulting in increased β -cell mass and improved glucose tolerance in diabetic rats. *Diabetes* 48:2270–2276
27. Zhou J, Wang X, Pineyro MA, Egan JM (1999) Glucagon-like peptide 1 and exendin-4 convert pancreatic AR42J cells into glucagon- and insulin-producing cells. *Diabetes* 48:2358–2366
28. Rolin B, Larsen MO, Gotfredsen CF et al (2002) The long-acting GLP-1 derivative NN2211 ameliorates glycemia and increases β -cell mass in diabetic mice. *Am J Physiol Endocrinol Metab* 283: E745–E752
29. Cernea S, Raz I (2011) Therapy in the early stage: incretins. *Diabetes Care* 34:S264–S271
30. Lahu G, Hünemeyer A, Diletti E et al (2010) Population pharmacokinetic modelling of roflumilast and roflumilast N-oxide by total phosphodiesterase-4 inhibitory activity and development of a population pharmacodynamic-adverse event model. *Clin Pharmacokinet* 49:589–606